Desalination and Water Treatment
www.deswater.com
doi: 10.5004/dwt.2020.24820

173 (2020) 427–441
January

Synthesis and characterization of ultrasonic-assisted *Delonix regia* seeds: modelling and application in dye adsorption

D. Sivakumar[a], R. Parthiban[b,*], P. Senthil Kumar[b,*], A. Saravanan[c]

[a]*Department of Chemical Engineering, Sri Venkateswara College of Engineering, Kancheepuram 602117, India, Tel: +919841929719; email: skumar@svce.ac.in*
[b]*Department of Chemical Engineering, SSN College of Engineering, Chennai 603110, India, Tel: +919884488302; email: parthibanr@ssn.edu.in (R. Parthiban), Tel. +919884823425; email: senthilchem8582@gmail.com (P. Senthil Kumar)*
[c]*Department of Biotechnology, Rajalakshmi Engineering College, Chennai 602105, India, Tel. +919003838356; email: sara.biotech7@gmail.com*

Received 2 May 2019; Accepted 25 August 2019

ABSTRACT

The adsorptive removal of malachite green (MG) dye using ultrasonic-assisted *Delonix Regia* seeds (UADRS) was studied in both experimental and theoretical studies. The physical and chemical characteristics of newly prepared adsorbent – UADRS were determined using scanning electron microscopy, Fourier-transform infrared spectroscopy, Brunauer–Emmett–Teller, thermogravimetric analysis and X-ray diffraction. The batch adsorption tests showed that adsorption was increasingly positive under the accompanying conditions: MG dye concentration = 50 mg L^{-1}, solution pH = 8.0, contact time = 60 min, dosage = 0.7 g L^{-1} and temperature = 30°C. Adsorption results were demonstrated to characterize fundamental parameters such as the adsorption equilibrium and kinetics. Equilibrium adsorption information was best obtained from the Freundlich isotherm model, and the maximum adsorption capacity was found to be 456.9 mg g^{-1}. The adsorption kinetic demonstrates a superior fit to the pseudo-first-order kinetic model. The adsorption thermodynamic investigations exhibited that adsorption was a chemisorption procedure with an exothermic and unconstrained sorption process. Sticking probability proclaimed that the present adsorption study was ideal at lower temperature and the sticking ability of MG dye onto UADRS was exceptionally high.

Keywords: Malachite green; *Delonix regia* seeds; Sticking probability; Isotherm; Thermodynamics

1. Introduction

Textile industries are majorly responsible for generating a large amount of wastewater due to different processing steps such as pre-treatment, bleaching, dyeing, printing, and finishing. Wastewater from a textile unit consists of many toxic pollutants such as dyes, detergents, color residues, inorganic salts, catalytic chemicals and stabilizing agents [1–3]. Textile industries directly discharge the untreated wastewater into the environmental water bodies, which causes several health issues to humans, animals, and plants. The environmental problems created by the textile industry wastewater are due to increased oxygen demand, high color, and a large number of suspended solids [4,5]. Also, textile dyes in high concentrations inhibit sunlight penetration, respiration activities and consequently upset the biological and photosynthesis processes in the aquatic environment [6–8]. Among the different dyes, malachite green (MG) is considered the most toxic, due to its respiratory toxicity, carcinogenic and mutagenic properties; it lasts for a long time in water and is difficult to be degraded by microorganisms [9,10]. Different physicochemical and

* Corresponding authors.

biological treatment strategies including ion exchange, precipitation, reverse osmosis, electrochemical treatment, ultrafiltration, and membrane separation have been accounted for to remove the toxic dyes from wastewater [11–19].

Nowadays, the adsorption process is the utmost favorable technique for the removal of organic and inorganic contaminants from the water environment. Adsorption technique has several advantages such as low cost, higher removal rate, regeneration of adsorbent and higher affinity towards the dye [8,20–24]. In the adsorption technique, several researchers have successfully implemented activated carbon (AC) as an effective adsorbent. AC has superior potential towards the dye removal due to its high surface area, adaptability and high porosity [25]. However, considering cost as a factor, agricultural waste biomass has been considered for the preparation of low cost-efficient adsorbent material for the removal of toxic dyes from the wastewater [26–33]. The agricultural waste biomass includes a cashew nutshell [34], tamarind seeds [35], cotton flower [36], peanut hull [37], rice husk [38], *Jatropha curcas* pods [39] and palm oil [40].

Adsorbents derived from naturally occurring agricultural biomass such as *Delonix Regia* seeds can be utilized for the removal of toxic dye from the water ecosystem. The novelty of the present research is to prepare an effective absorbent – ultrasonic-assisted *Delonix Regia* seeds (UADRS) for the effective removal of MG dye. The adsorption of MG dye was examined using raw *Delonix Regia* seeds. Due to its low surface area and porosity, UADRS was synthesized and adapted, to modify the surface of *Delonix Regia* seeds. The external morphology and the structure of the incorporated adsorbent material were portrayed by different systems, for example, Fourier-transform infrared spectroscopy (FTIR), scanning electron microscopy (SEM), Brunauer–Emmett–Teller (BET), thermogravimetric analysis (TGA) and X-ray diffraction (XRD). The parameters such as MG dye concentration, pH, contact time, adsorbent dose and temperature were studied by batch adsorption study. The adsorption process, rate, and mechanism were predicted by the adsorption isotherm model and adsorption kinetic model, respectively. The thermodynamic examinations were performed to perceive the nature of the adsorption process.

2. Materials and methods

2.1. Collection and preparation of adsorbent

In this study, *Delonix regia* seeds were utilized as an adsorbent for the removal of MG dye from the aqueous solution. The *Delonix regia* seeds were collected from different farm fields near Thiruporur, Tamilnadu, India. The collected seeds were washed continuously using distilled water to remove the dust particles. The samples were dried in an oven at the temperature of 80°C for about 6 h to remove the total dampness content. These dried samples were pulverized to residual form and gathered in a plastic dish for corrosive treatment. 0.1 M hydrochloric acid (HCl) was added to the sample where it stayed for around 5 h. The surface-modified material was washed using refined water to remove the abundant measure of HCl present in it. It was washed until the pH of the water wound up nonpartisan. At that point, the adsorbent was permitted to dry for around 24 h at 60°C in a hot air oven. The resultant material was further utilized for the preparation of UADRS. The ultrasonication was done with an ultrasonicator (Sonics Materials Inc., Newtown, USA) at a waged recurrence of 24 kHz and a motorized tumult of 500 rpm for around 1 h. The resultant material was sifted by using the Whatman 42 filter paper. The filtered material was dried at 40°C for around 24 h. The subsequent material was called ultrasonic aided *Delonix regia* seeds and it was viably utilized as an adsorbent material for the expulsion of MG dye from the aquatic environment.

2.2. Preparation of absorbate

MG dye, a crystalline powder (molecular formula: $C_{23}H_{25}ClN_2$; λ_{max} = 618.32 nm; molecular weight: 364.911) was purchased from E. Merck, India. The stock arrangement of 1,000 mg L^{-1} of MG dye was set up by softening the obligatory measure of MG dye crystal-like powder in 1,000 mL of refined water. The readied stock arrangement was debilitated by utilizing distilled water to achieve the waged arrangement of various MG dye concentrations (50–250 mg L^{-1}). The pH of the solution was changed by fitting an incentive by including 0.1 N NaOH or 0.1 N HCl. The pH of the arrangement was determined with Hanna pH meter (HI 98107, Hanna equipment Pvt. Ltd., Mumbai, India) utilizing a joined glass cathode.

2.3. Characterization study

The characterization of newly prepared UADRS was determined by different studies such as FTIR, SEM, BET, TGA, and XRD. FTIR studies can be used to determine the functional groups present on the surface of the adsorbent material. Furthermore, the nature of the interaction between the UADRS and MG dye was determined. SEM investigation can be utilized to decide the surface morphology of UADRS. BET investigation can be utilized to decide the surface property of UADRS. TGA analysis can be used to determine the thermal stability of the UADRS. XRD analysis can be used to identify the different phases of UADRS.

2.4. Batch adsorption experiments

Batch adsorption experiments were carried out for different factors influencing parameters such as concentration of MG dye (50–250 mg L^{-1}), contact time (10–90 min), pH (2.0–10.0), dosage of adsorbent (0.1–0.8 g L^{-1}) and temperature (30°C–60°C) to understand the rate of adsorption of MG dye from the synthetic solution. In each examination, the fixed amount of UADRS was included in the 100 mL flask, which comprises of 100 mL of MG dye solution. The mixtures were disturbed at 80 rpm in an incubation shaker (Orbitek, India) through various time intervals. After the prescribed time interval, the samples were retrieved from the shaker and the adsorbent material was filtered by using Whatman 42 filter paper. The MG dye concentration in the arrangements was estimated using a UV Visible spectrophotometer (JASCO, USA). The removal rate of the MG dye was determined by making use of the accompanying condition:

$$\text{Percentage removal} = \frac{C_0 - C_e}{C_e} \times 100 \quad (1)$$

where C_0 is the initial pollutant concentration (mg L^{-1}) and C_e is the final pollutant concentration in the solution (mg L^{-1}).

2.5. Isotherm study

The adsorption isotherm plays an important role in the evaluation of the interaction between the adsorbent surface at equilibrium condition and the dispersion of the MG dye in the solution. The batch adsorption study was carried out by changing the concentration of MG dye from 50 to 250 mg L^{-1}. A fixed amount of UADRS was included in each conical flask, which comprises 100 mL of various concentrations of MG dye at an ideal condition. When the framework achieved the equilibrium time, the samples were retrieved from the shaker. The expended UADRS was recuperated from arrangement blends by using the Whatman 42 channel paper. The concentration of the MG dye in the filtrate was analyzed by using UV Visible spectrophotometer. The measure of MG dye adsorbed onto the UADRS at a parity-time was controlled by using the accompanying mass equality condition:

$$q_e = \frac{\left(C_0 - C_e\right)V}{m} \quad (2)$$

where q_e is the adsorption capacity at equilibrium (mg g^{-1}), V is the volume of pollutant solution (g) and m is the mass of UADRS (g).

Four experimental isotherm models such as Langmuir, Freundlich, Temkin, and Toth model, defined the performance of the UADRS for the removal of MG dye from the aqueous solution.

Langmuir model can be described by the following equation [41]:

$$q_e = \frac{q_m K_L C_e}{1 + \left(K_L C_e\right)} \quad (3)$$

where q_m is the maximum monolayer adsorption capacity (mg g^{-1}), and K_L (L mg^{-1}) is the Langmuir constant related to the affinity of the dyes to the adsorbent.

Freundlich model can be described by the following equation [42]:

$$q_e = K_F C_e^{\frac{1}{n}} \quad (4)$$

where K_F ((mg g^{-1})(L mg^{-1}))$^{-1/n}$ is the Freundlich constant used to measure the adsorption capacity, and $1/n$ is a dimensionless parameter, which shows how adsorption fluctuates as an element of the concentration.

Temkin model can be described by the following equation [43]:

$$q_e = \frac{RT}{b}\left(\ln A\, C_e\right) \quad (5)$$

where A and B are the Temkin isotherm constants.

Toth model can be described by the following equation [44]:

$$q_e = \frac{q_{\mathrm{mT}} C_e}{\left(\frac{1}{K_T} + C_e^{\mathrm{mT}}\right)^{\frac{1}{\mathrm{mT}}}} \quad (6)$$

where K_T is the Toth equilibrium consistent, mT is the Toth demonstrate exponent and q_{mT} is the Toth greatest adsorption limit (mg g^{-1}).

2.6. Kinetic study

The kinetic investigations were coordinated to investigate the removal rate and mechanism for the removal of MG dye by UADRS. The adsorption kinetic examinations were finished by changing the contact time (10–90 min) and at an ideal condition of initial MG dye concentration = 50 mg L^{-1}, pH = 8.0, temperature = 30°C, adsorbent measurements = 0.5 g L^{-1} of UADRS. When the framework achieved the harmony time, the samples were returned from the shaker. The expended UADRS was recuperated from arrangement blends by utilizing the Whatman 42 channel. The leftover MG dye concentration in the filtrate was investigated by utilizing a UV Visible spectrophotometer. The proportion of MG dye adsorbed at different time intervals (q_t mg g^{-1}) was figured using the formula:

$$q_t = \frac{\left(C_0 - C_t\right)V}{m} \quad (7)$$

where q_t is the pollutant concentration in the solid phase at any time t (mg g^{-1}), C_t is the pollutant concentration at time t (mg L^{-1})

Pseudo-first-order kinetic model is expressed as follows [45]:

$$q_t = q_e\left(1 - \exp\left(-k_1 t\right)\right) \quad (8)$$

where k_1 is the pseudo-first-order kinetic rate constant (min^{-1}) and t is the time (min).

Pseudo-second-order kinetic model is expressed as follows [46]:

$$q_t = \frac{q_e^2 k_2 t}{1 + q_e k_2 t} \quad (9)$$

where k_2 is the pseudo-second-order kinetic rate constant (g min^{-1} mg^{-1}) and t is the time (min).

Elovich kinetic model is expressed as follows [47]:

$$q_t = \left(1 + \beta_E\right)\ln\left(1 + \alpha_E \beta_E t\right) \quad (10)$$

where β_E (g mg^{-1}) is the desorption consistent identified with the enactment vitality of chemisorption and α_E is the underlying adsorption rate (mg g^{-1} min^{-1}).

2.7. Thermodynamic study

The thermodynamics studies were carried out by differing the temperature from 30°C to 60°C to get the data about the vitality deviations. The thermodynamic paradigm was clarified by the thermodynamic constraints, such as Gibbs free energy ($\Delta G°$, kJ mol^{-1}), entropy change ($\Delta S°$, kJ mol^{-1}) and enthalpy change ($\Delta H°$, kJ mol^{-1}). The thermodynamic parameters were determined from the accompanying conditions:

$$\Delta G° = -RT\ln K_c \tag{11}$$

$$K_c = \frac{C_{\text{Ae}}}{C_e} \tag{12}$$

$$\log K_c = \frac{\Delta S°}{2.303R} - \frac{\Delta H°}{2.303RT} \tag{13}$$

where R is the universal gas constant (8.314 JK mol^{-1}), T is the temperature (K), K_c is the equilibrium constant. C_{Ae} is the amount of MG dye adsorbed onto the adsorbent (UADRS) per liter of MG dye solution at equilibrium (mg L^{-1}). The estimations of $\Delta S°$ and $\Delta H°$ were resolved from the incline esteem and the catch estimation of the plot between of log K_c and $1/T$.

2.8. Single stage batch adsorber

Adsorption isotherm study assumes an imperative part in the design of a single-stage batch adsorption system. The motivation behind the configuration is to estimate the amount of adsorbent dosage expected to treat the known volume of the effluent. The best-obeyed adsorption isotherm model was utilized to outline a single-stage batch adsorption system.

2.9. Sticking probability

The sticking probability (S^*) was used to determine the sticking capacity of MG dye to remain adsorbed indeterminately. The sticking probability can be calculated by using the following formula

$$S^* = (1-0)\exp\left(-\frac{E_a}{RT}\right) \tag{14}$$

θ represents that surface coverage, E_a represents that activation energy. The surface coverage was evaluated by utilizing the following condition

$$0 = 1 - \frac{C_e}{C_0} \tag{15}$$

3. Results and discussion

3.1. Characterization studies

3.1.1. FTIR Studies

The surface chemistry of the adsorbent material plays an important role in determining the adsorption mechanism. The FTIR analysis might be connected to locate the organic and inorganic materials present on the surface of the UADRS. The adsorption component is completely subject to the communication amid the MG dye and the UADRS. The FTIR study annals the ranges from a maximum point of confinement of around 4,000 cm^{-1} down to 400 cm^{-1}. Fig. 1a demonstrates that FTIR examination of UADRS. In Fig. 1a the extraordinary wide band at 1,582 cm^{-1} demonstrates the nearness of aromatic ring stretch (C=C–C) of aryl group and the band vibrations at 558 and 529 cm^{-1} relates to the nearness of aliphatic organohalogen compound group frequencies of aliphatic-iodo compounds (C–I Stretch). The pinnacle vibrations at 495 and 476 cm^{-1} demonstrates the nearness of thiol group frequencies of polysulphides (S–S Stretch). The extreme tops at 455 and 427 identify with that of the quality of aryl disulfides (S–S Stretch). The FTIR report reports that the carbonate ion was present in the peak value at 443 cm^{-1} that indicates that the stretching vibrations of ionic groups. The FTIR considers detailed that the nearness

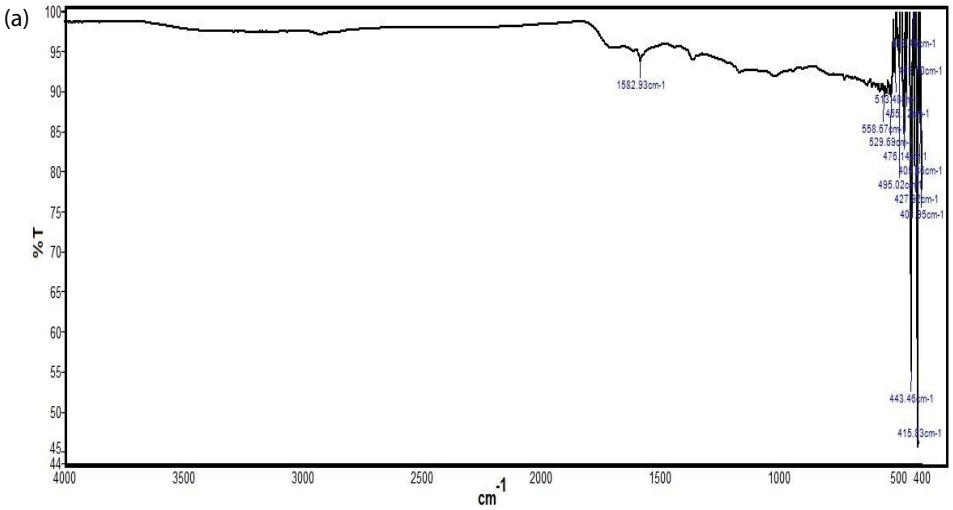

Fig. 1. (*Continued*)

(b)

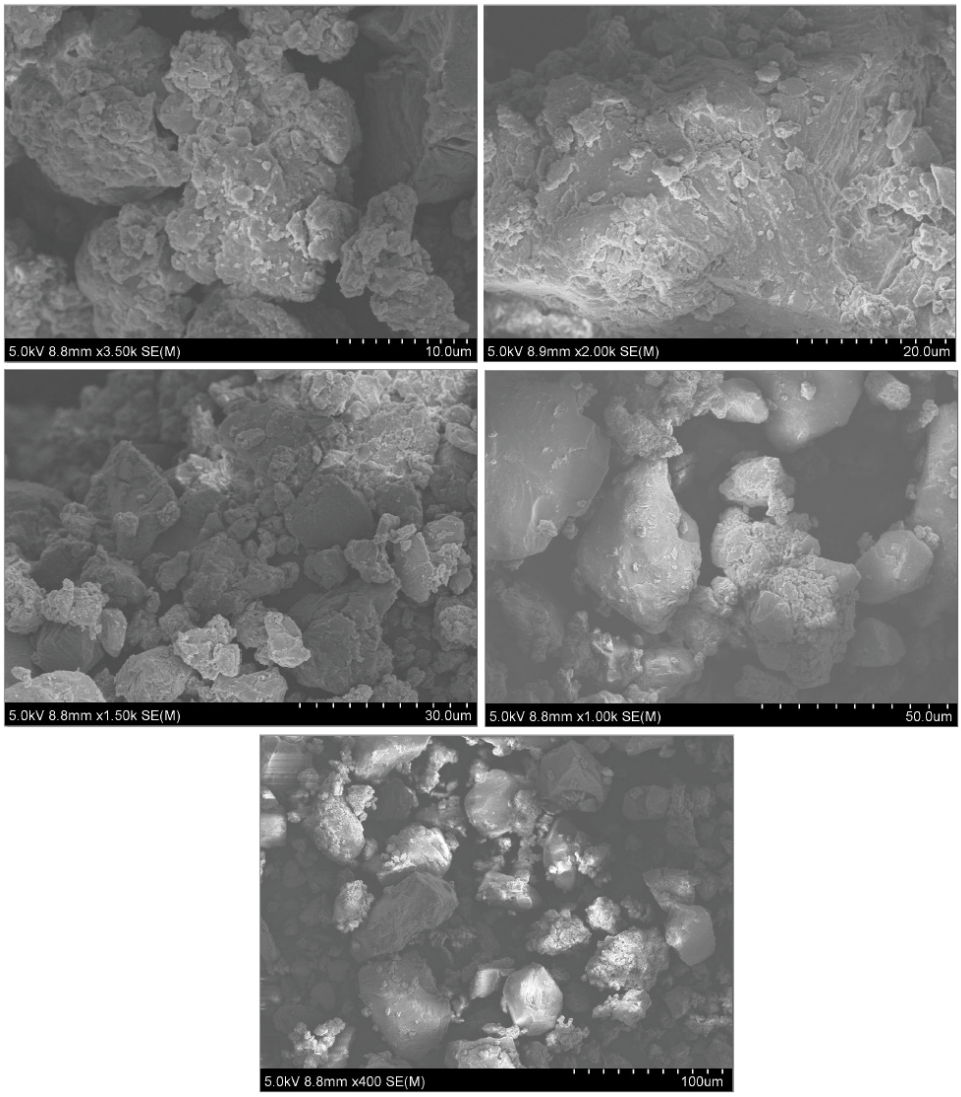

(c)

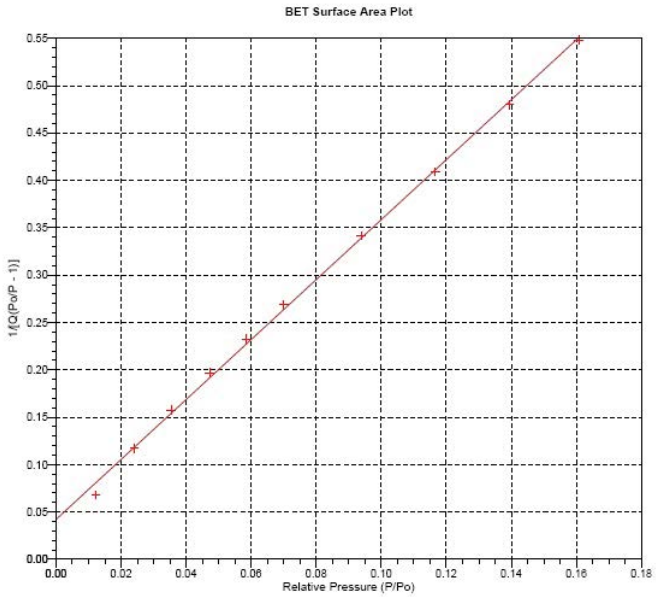

Fig. 1. (*Continued*)

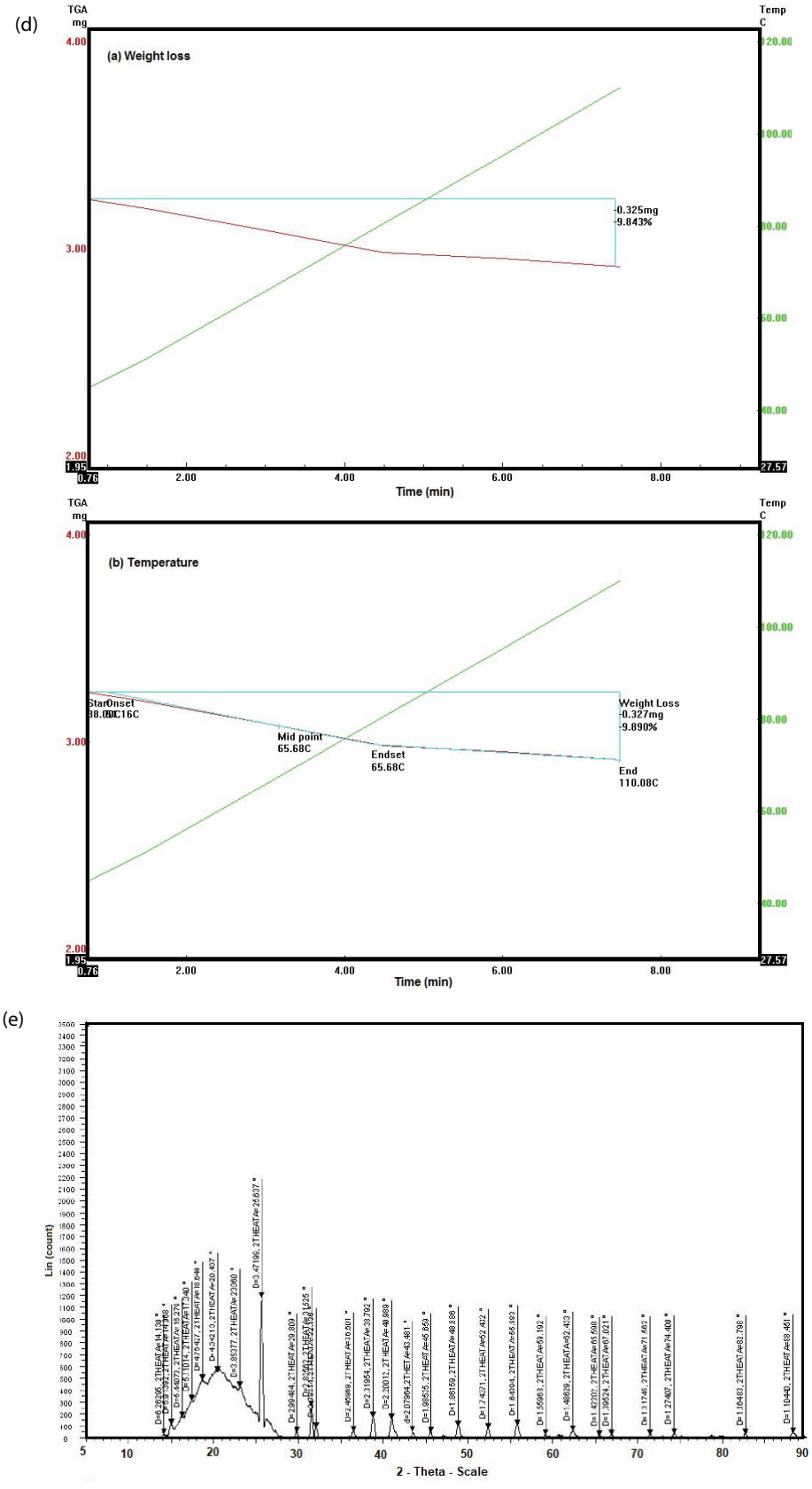

Fig. 1. (a) FTIR image of UADRS, (b) SEM analysis of UADRS, (c) BET analysis of UADRS, (d) TGA analysis of UADRS, and (e) XRD image of UADRS.

of the aryl group is in charge of the development of bond collaboration (electrostatic and covalent) amid the MG dye and the UADRS. The presence of ionic groups might be the major reason for the formation of a covalent bond between the UADRS and MG dye. The nearness of the aliphatic cluster is responsible for the arrangement of the framework with a fractious connected arrange because of its developed thickness afterward alteration. FTIR results showed that the presence of thiol, aryl, ionic groups, covalent and electrostatic interaction confirms that UADRS has good adsorption capacity for the removal of MG dye.

3.1.2. SEM analysis

The exterior form, shape, and structure of UADRS was revealed by the SEM images with different magnifications of 8.8 mm of ×3,500 and 10 μm, 8.9 mm of ×2,000 and 20 μm, 8.8 mm of ×1,500 and 30 μm, 8.8 mm of ×1,000 and 50 μm, 8.8 mm of ×400 and 100 μm, respectively. Fig. 1b demonstrates the homogeneous and generally permeable structure in the UADRS. The isolated pores of varying dimensions from micro to transitional pores. Layers of carbon that are interconnected are seen. The structures signify the presence of macropores very clearly and it is responsible for the high surface area of UADRS. The proximity of the tremendous level of a surface area and size of pores might be a direct result of the take-up of water particles and the closeness of void volume outwardly of the adsorbent material during ultrasonication process. SEM analysis reported that UADRS has a good number of pores and large cavities, which will enhance the adsorption capacity by forming the matrix layer with a cross-linked network. These qualities exhibit that UADRS has an overwhelming adsorption limit concerning the clearing of MG dye from the fluid arrangement.

3.1.3. BET analysis

BET analysis can clear up the surface adsorption of MG dye on a solid surface of a UADRS. BET is a fundamental examination for the estimation of the specific surface area of the adsorbent. The surface area can be used to predict bioavailability. The effect of the total surface area is a fundamental aspect of the adsorption process. Fig. 1c shows the BET surface area tests for UADRS. BET surface area, pore-volume, correlation coefficient and molecular cross-sectional area of UADRS were observed to be 1.3579 $m^2\ g^{-1}$, 0.003620 $cm^3\ g^{-1}$, 0.9993499 and 0.1620 nm^2, exclusively. BET results showed that present adsorbent material – UADRS has enlarged pore volume and efficient molecular cross-sectional area, which shows that superior adsorption capacity for the removal of MG dye from the aqueous solution.

3.1.4. TGA analysis

TGA is an analytical technique used to determine a UADRS's thermal stability and its fraction of volatile components by monitoring the weight change that occurs as a sample is heated at a constant rate. Fig. 1d shows the TGA twist of UADRS using an SDT Q600 V8.0 instrument. The TGA examination of UADRS found in the temperature district of 70°C–85°C created the impression that 9.89% of weight adversities, as a rule, result in the vaporization of water and period of non-combustible gases. In the TGA examination, the couple of cellulosic macromolecules of UADRS, for instance, glucose, xylose, mannose, galactose and arabinose experience pyrolysis movement and get vaporized. As shown by the TGA examination, the adsorbent material has a midpoint estimation of 65.68°C and an end set estimation of 110.08°C. Over this temperature, the UADRS will be corrupted. The expansion in thermal stability of joined cellulosic fiber might be because of the fuse of increasingly covalent bonding. The grafted item shaped a cross-linked sort of system on the cellulosic macromolecules. When heated forms an insulative carbonaceous char boundary superficially, along these lines restraining corruption and thus expands thermal dependability of united cellulosic macromolecules.

3.1.5. XRD analysis

Fig. 1e demonstrates the XRD image of UADRS. The crystal-like idea of the mixes was controlled by utilizing the procedure of XRD. The solid diffraction of UADRS was seen in the situation of 2θ that proposes that UADRS shows an orthorhombic crystal structure. The presence of aryl functional groups (558 cm^{-1}) and thiol functional groups (495 cm^{-1}) on the surface of the UADRS were affirmed by FTIR studies. These functional groups were in charge of ascending in the crystallinity record from the solid hydrogen holding. The diffraction file of UADRS was less extraordinary and crystallinity record likewise diminished, as it were, as appears in Fig. 1e. From that point forward, the crystallinity was diminished, as it were, in which electrostatic association framed by aryl utilitarian mixes affirmed. In like manner, the XRD study of UADRS detailed that UADRS has supplementary adsorption locales. This approach can provide not only a quantitative estimation of the UADRS phases but also some useful information on the sorbent structure and microstructure such as lattice parameters, average crystallite size, and microstrain. Subsequently, the XRD considers point by point that UADRS material has an incredible adsorption limit concerning MG dye adsorption from the aqueous solution.

3.2. Influence of initial MG dye concentration on the MG dye adsorption

Fig. 2a displays the impact of MG dye concentration on the adsorption of MG dye onto UADRS. The impact of initial MG dye concentration was analyzed by varying the MG color focus from 50 to 250 mg L^{-1}. It was seen that the percentage removal of MG dye was diminished with an expansion of MG dye concentration. This might be because of the immersion of the accessible dynamic destinations on the adsorbent surface. At a lower MG dye concentration, the proportion of adsorbent to MG dye concentration was at most extreme, demonstrating higher MG dye evacuation at lower MG dye concentration. At higher MG dye concentration, the proportion of adsorbent to MG dye concentration was at least, showing lower MG dye concentration. In any case, practically 100% of MG dye was removed from the aquatic medium, indicating that the UADRS can be used as

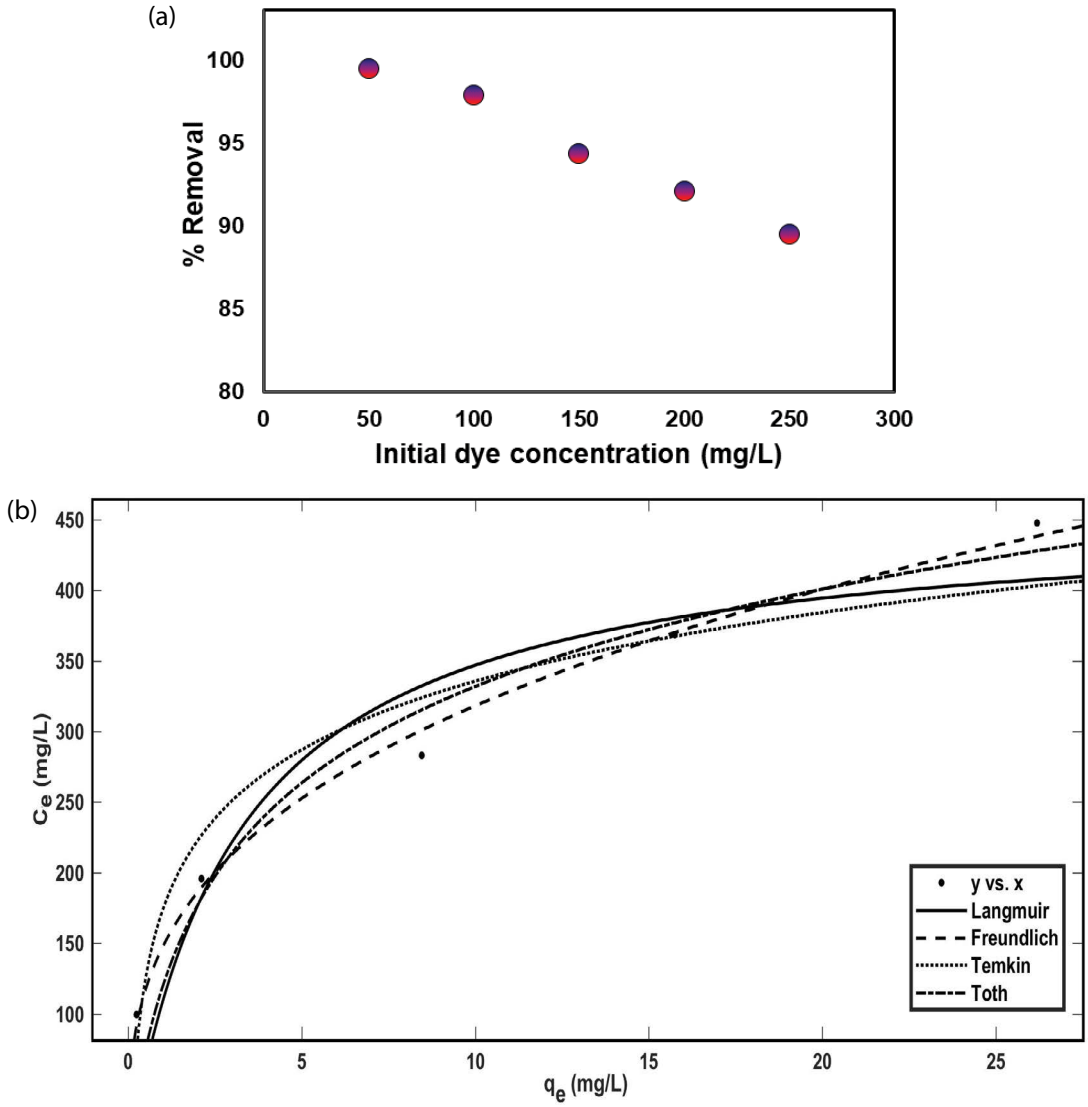

Fig. 2. (a) Initial MG dye concentration effect on the adsorption of MG dye onto UADRS and (b) Adsorption isotherm fit for the removal of MG dye onto UADRS.

an overwhelming adsorbent for the incredible removal of MG dye from the fluid arrangement.

3.3. Isotherm study

Isotherms have a basic impact in prescient demonstrating methods, which are utilized for the development of adsorption framework. Adsorption equilibrium information was fitted with the distinctive isotherm conditions and anticipated pictures are exhibited in Fig. 2b. The determined adsorption isotherm parameters, correlation coefficient (R^2) qualities and error esteems are recorded in Table 1. The best-fitted adsorption models can be distinguished by either R^2 qualities or error values. Freundlich isotherm ($R^2 = 0.9933$) gives the best outcome to the adsorption framework as looked at with the other isotherm models. This reveals insight into the character of the adsorption process; here it is portrayed by the multilayer adsorption process. The estimation of n was observed to be more noteworthy than one, which demonstrates the MG dye adsorption onto UADRS was physical adsorption.

3.4. Influence of the contact time on the MG dye adsorption

Fig. 3a demonstrates the impact of contact time on the adsorption of MG dye onto UADRS. The effect of contact time on the adsorption of MG dye onto UADRS was carried out by fluctuating the contact time from 10 to 90 min and possession distinctive constraints as steady. Fig. 3a shows that the rate of removal of MG dye was extended with the development of contact time from 10 to 60 min and additional elevation in time has no noticeable outcome on MG dye adsorption. The motive might be that at introductory a liberal superficial assortment stretches plentiful superficial unique locale to MG dye adsorption be that as it may, over the long haul UADRS surface may have been

Table 1
Isotherm results for the adsorption of MG dye onto UADRS

Isotherm model	Parameters	R^2	SSE	RMSE	Equation
Langmuir	q_m = 456.9 (mg g^{-1}) K_L = 0.3155 (L mg^{-1})	0.8818	9.35	5.58	$q_e = \frac{456.9 \times 0.3155 \times C_e}{1 + 0.3155 \times C_e}$
Freundlich	K_F = 147.9 ((mg g^{-1})(L mg^{-1})$^{(-1/n)}$) n = 3.006 (g L^{-1})	0.9933	5.88	1.02	$q_e = 147.9 \times C_e^{\frac{1}{3.006}}$
Temkin	A = 12.01 b = 3.621	0.9302	12.01	3.621	$q_e = \frac{0.3638 \times T}{3.621}\left[\ln\left(12.01 \times C_e\right)\right]$
Toth	q_{mT} = 30.2 (mg g^{-1}) K_T = 0.859 m_T = 0.8923	0.9338	50.26	50.03	$q_e = \frac{30.2 \times C_e}{\left[\frac{1}{0.859} + C_e^{0.8923}\right]^{\frac{1}{0.8923}}}$

depleted accomplishing no supplementary removal process. No huge expansion in rate launch was searched for all tried MG dye focus after 60 min of contact time; this shows the parity-time was fixed as 60 min for additionally endeavors.

3.5. Kinetic study

The kinetic study for the adsorption of MG dye on UADRS performance fundamental employment in the removal study, which gives information about the reaction lane and the proportion monitoring instrument of exchange reactions. The adsorption rate and the dynamic instrument of the adsorption technique were assessed by using the adsorption active examination. In the present investigation, kinetic models were fitted with the exploratory information to assess the finest dynamic model. Fig. 3b demonstrates the adsorption kinetic investigations on MG dye adsorption by UADRS. The determined estimations of kinetic constraints R^2 and sum of squared error (SSE), root mean squared error (RMSE) appear in Table 2. The finest model was recognized by contrasting the trial adsorption esteem ($q_{e,\exp}$) with the determined adsorption limit ($q_{e,\text{cal}}$). It is seen from Table 2 that the determined adsorption limit esteems ($q_{e,\text{cal}}$) of pseudo-first-order were nearest to the test adsorption limit ($q_{e,\exp}$). Additionally, the pseudo-first-order model demonstrates had a superior fit to the exploratory information contrasted with other active models, considering the higher relationship coefficient esteems and low SSE and RMSE it appeared. In perspective on all these, it very well may be presumed that the pseudo-first-order kinetic model can around depict all adsorption of MG dye on UADRS. This likewise proposes removal study is constrained by physical adsorption including the development of bonding forces (covalent, Vander Walls) between MG dye and the superficial of the UADRS.

Table 2
Kinetic results for the adsorption of MG dye onto UADRS

Kinetic model	Parameters	MG dye Concentration (mg L^{-1})				
		50	100	150	200	250
Pseudo-first-order	k_1 (min^{-1})	0.0398	0.0346	0.0315	0.0268	0.022
	$q_{e,\text{cal}}$ (mg g^{-1})	105.3	212.4	314.7	427.9	554.4
	$q_{e,\exp}$ (mg g^{-1})	99.85	195.92	284.9	370.89	449.56
	R^2	0.9846	0.9818	0.9801	0.9781	0.9674
	SSE	6.91	33.1	86.8	192.2	253.0
	RMSE	3.022	6.934	11.15	16.57	26.64
Pseudo-second-order	k_2 (g mg^{-1} min^{-1})	0.0387	0.0313	0.0264	0.0210	0.0159
	$q_{e,\text{cal}}$ (mg g^{-1})	11.61	16.76	20.66	24.64	28.77
	R^2	0.9753	0.9705	0.9674	0.966	0.9574
	SSE	10.5	55.0	142.6	298.4	650.3
	RMSE	3.827	8.864	14.27	20.65	30.48
Elovich Kinetic	α_E (mg g^{-1} min^{-1})	0.0144	0.0042	0.0020	0.0008	0.0003
	β_E (g mg^{-1})	14.53	33.79	54.71	85.11	126.6
	R^2	0.9589	0.956	0.953	0.9533	0.9475
	SSE	17.5	82.2	205.6	409.7	800.4
	RMSE	4.936	10.83	17.14	24.19	33.82

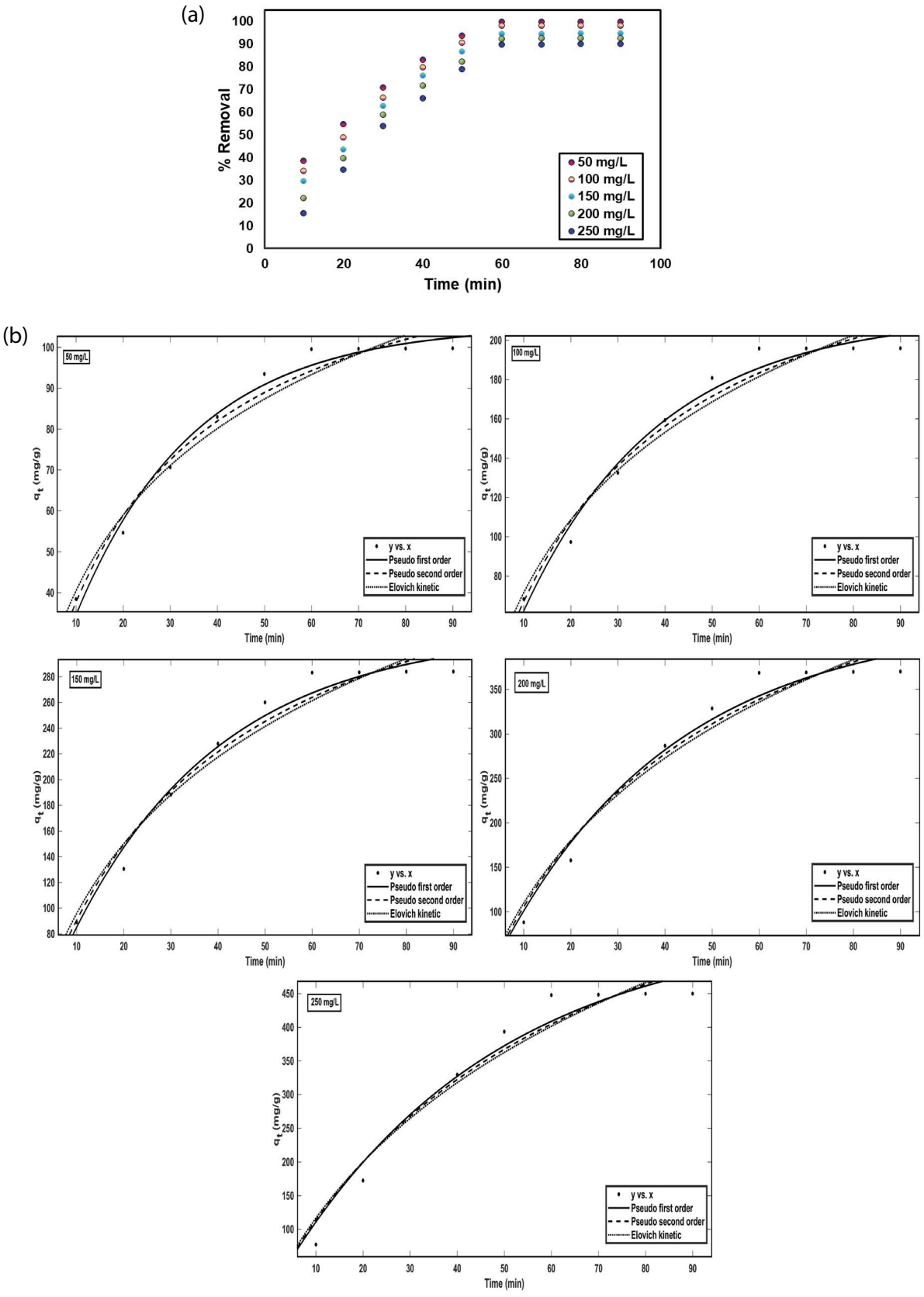

Fig. 3. (a) Contact time effect on the adsorption of MG dye onto UADRS and (b) Adsorption kinetic fit for the removal of MG dye onto UADRS.

The pseudo-first-order kinetic model infers that the quantity of adsorption destinations that were available superficially of the UADRS is broadly more prominent than the quantity of MG dyes that were adsorbed.

3.6. Influence of the pH on the MG dye adsorption

Fig. 4, demonstrates the impact of pH on the adsorption of MG dye onto UADRS. The impact of pH study was performed by shifting the arrangement pH from 2.0 to 10.0 and keeping other parameters as steady. The adsorption blends were worked under ideal conditions in an incubation shaker for 60 min. The underlying grouping of MG dye was kept up at 50 mg L^{-1}. The removal rate of MG dye was gradually expanded with the expansion in pH esteem. The extreme expulsion of MG dye was seen at a pH estimation of 8.0. Low expulsion of MG dye by the UADRS was seen at truncated pH esteem, which might be expected to the developed grouping of hydrogen particles contending with the MG dye to be adsorbed onto the UADRS. At higher pH esteem (pH ≥ 8.0), the evacuation of MG dye was accomplishing the immersion condition due to the arrangement of metal hydroxides. The last estimations of the arrangement pH were observed to be underneath 9.0, which shows that no precipitation happens amid the adsorption procedure.

3.7. Influence of UADRS dosage on the MG dye adsorption

Fig. 5 demonstrates the impact of dose on the adsorption of MG dye onto UADRS. The effect of adsorbent dose was considered by shifting the measurement from 0.1 to 0.8 g L^{-1} and keeping different parameters as consistent. The working conditions used for the present examination were introductory MG dye concentration of 50 mg L^{-1}, arrangement pH of 8.0, the contact time of 60 min and temperature of 30°C. This outcome demonstrates that the evacuation of MG dye was expanded gradually with the expansion of the adsorbent portion from 0.1 to 0.5 g L^{-1}, due to the expansion in the number of dynamic destinations on the UADRS superficial. As the UADRS portion increments further from 0.5 to 0.8 g L^{-1}, the rate of removal of MG dye came to almost a steady esteem. This is conceivable because of the moderately low equilibrium concentration, low driving drive, and the accessible dynamic locales bit by bit diminished. The ideal measurements of UADRS for the expulsion of MG dye were observed to be 0.5 g L^{-1}.

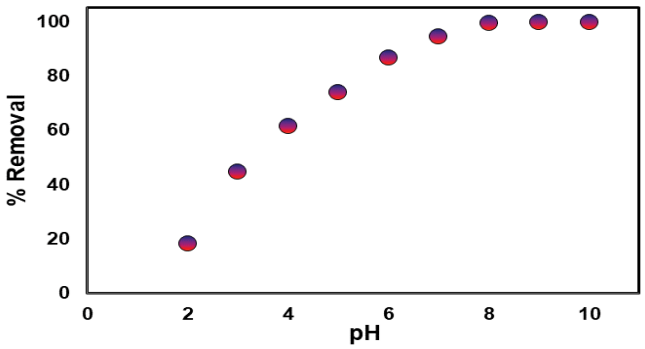

Fig. 4. Solution pH effect on the adsorption of MG dye onto UADRS.

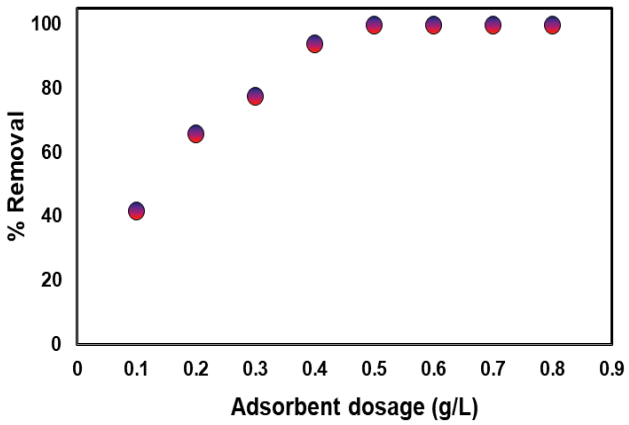

Fig. 5. Dosage effect on the adsorption of MG dye onto UADRS.

3.8. Influence of temperature on the MG dye adsorption

Fig. 6a shows the impact of temperature on the present removal study. The temperature impact on the expulsion of MG dye was thought about by moving the temperature running from 30°C to 60°C and by maintaining each other parameter constant. The working conditions used for the present examination were MG dye centralization of 50 mg L^{-1}, contact time 60 min, pH of 8.0 and UADRS bit of 0.5 g L^{-1}. The expulsion of MG dye from the liquid course of action was reduced with an extension in the temperature, which exhibited that the adsorption progression was exothermic. Temperature is related to the dynamic imperativeness of the dyes in the liquid plan. As temperature increases, physical mischief may occur on the adsorbent material and diminish its adsorption limit; this might be possibly a direct result of the weakening of adsorptive powers between the MG dye and the UADRS. The extraordinary departure of MG dye was accomplished at 30°C.

3.9. Thermodynamic study

Fig. 6b shows the thermodynamic examination for the adsorption of MG dye onto UADRS. The estimations of enthalpy and entropy were resolved from the incline and intercept of the plot of ln K_c vs. 1/T, separately. The evaluated constraints are documented in Table 3. From the tabulation report, negative estimations of $\Delta G°$ for every one of the obsessions were very much arranged reached out with an extension of temperature from 303 to 333 K which relates that adsorption of MG dye onto UADRS was functional and unconstrained. The reason behind this direct, the increase of temperature improved the advancement of MG dye ahead of time adsorbed, which made a case of desorption of the MG dye from the UADRS surface. In the present framework, $\Delta G°$ respect was found in the focal point of –20 to 0 kJ mol^{-1} for all contemplated temperature which displays that present adsorption of MG dye onto UADRS was physical adsorption. The negative estimations of $\Delta H°$ address that adsorption of MG dye onto the UADRS was exothermic. Likewise, negative estimations of $\Delta S°$ showed diminished irregularity at the solid/fluid interface amidst the adsorption procedure.

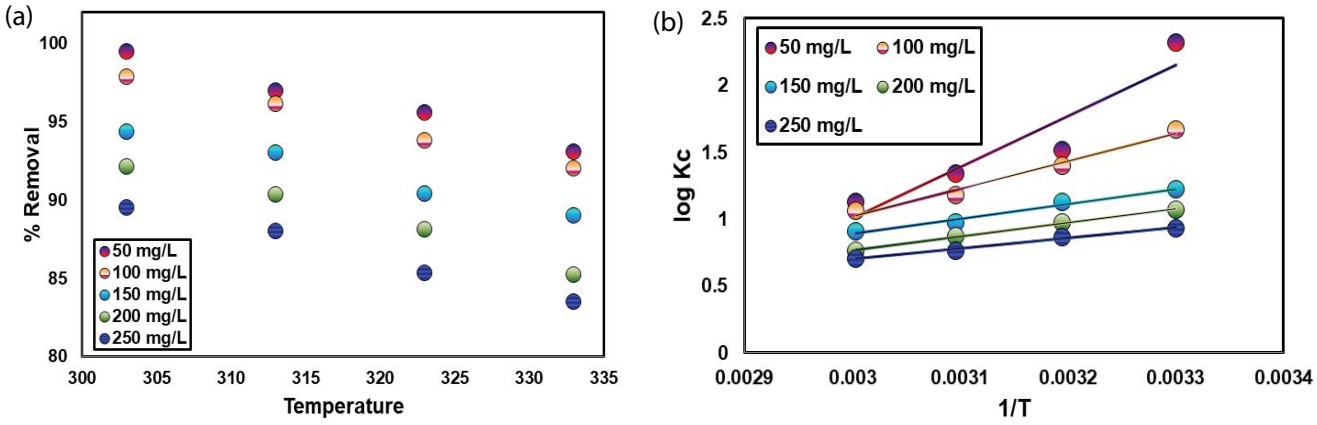

Fig. 6. (a) Temperature effect on the adsorption of MG dye onto UADRS and (b) Thermodynamic study.

Table 3
Thermodynamic parameters for the removal of MG dye using UADRS

Concentration. of MG dye (mg L^{-1})	$\Delta H°$ (KJ mol^{-1})	$\Delta S°$ (J mol^{-1} K^{-1})	$\Delta G°$ (KJ mol^{-1})			
			30°C	40°C	50°C	60°C
50	–73.027	–199.73	–13.469	–9.066	–8.287	–7.214
100	–39.356	–98.49	–9.668	–8.375	–7.314	–6.771
150	–21.176	–46.41	–7.097	–6.745	–6.034	–5.792
200	–19.698	–44.44	–6.195	–5.824	–5.382	–4.855
250	–15.110	–31.93	–5.404	–5.193	–4.728	–4.494

3.10. Single stage batch adsorber

A schematic diagram for a solitary stage batch adsorber arrangement is shown in Fig. 7. The essential point of this planned design is to decrease the MG dye concentration from C_0 to C_e of plan volume V (L). The proportion of UADRS used is M (g), and the MG color adsorbed onto the UADRS was changed from q_0 (mg g^{-1}) to q_e (mg g^{-1}).

The mass adjustment for the single-sort out gathering adsorption structure at parity condition can be given as seeks after (at time $t = 0$, $q_0 = 0$):

$$V\left(C_o - C_e\right) = M\left(q_e - q_o\right) = Mq_e \tag{16}$$

Freundlich isotherm shows the best-fitted model adsorption isotherm appear for the MG dye onto the UADRS. The single-organize clump adsorber was arranged by using the Freundlich adsorption isotherm appear. Updating the Eq. (15) can be given as seeks after

$$M = \frac{\left(C_0 - C_e\right)}{q_e}V = \frac{\left(C_0 - C_e\right)}{K_F C_e^{\frac{1}{n}}}V \tag{17}$$

Fig. 7 demonstrates the straight conspiracy of the measure of adsorbent (g) vs. volume of the arrangement of starting MG dye concentration (L) of 300 mg L^{-1} for 75%, 80%, 85%, 90% and 95% of expulsion at various arrangement volumes (1–10 L).

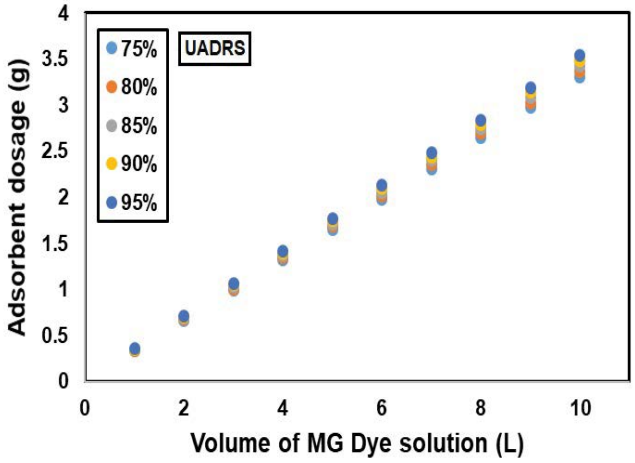

Fig. 7. Pictorial representation of single-stage batch adsorber.

3.11. Sticking probability

The estimations of staying likelihood (S^*) and actuation vitality (E_a) are shown in Table 4. The estimations of S^* were seen that underneath 1, subsequently the staying likelihood of MG dye onto the UADRS is high and besides negative estimation of E_a analyzes that adsorption of MG dye particle onto UADRS was continuously extraordinary at the lower course of action temperature. Thus, the adsorption process was exothermic.

3.12. Comparison of adsorption capacity of UADRS

Assorted adsorption studies about utilizing distinctive kinds of adsorbent materials for the evacuation of MG dye have been accounted for. The most extraordinary monolayer adsorption points of confinement of UADRS were differentiated and various adsorbent materials and the result are listed in Table 5. The report shows that UADRS has a higher adsorption limit 456.9 mg g^{-1} that exhibited that UADRS is to be considered as promising and effective adsorbent material for the ejection of MG dye from the contaminant liquid.

4. Conclusion

In this study, *Delonix regia* seeds were synthesized via ultrasonic technique and utilized as an adsorbent material for the adsorption of MG dye from the aqueous solution. The newly synthesized UADRS was characterized by FTIR, SEM, BET, TGA and XRD analysis. The characterization reports expressed that the prepared adsorbent had sufficient external possessions for the expulsion of MG dye. The adsorption isotherm examines demonstrate that Freundlich isotherm display fitted great with the exploratory information which depicts that the present research is heterogeneous. The monolayer adsorption limit for the expulsion of MG dye was observed to be 456.9 mg g^{-1}. Kinetics and thermodynamic analyses showed that the MG dye adsorption process was chemisorption, impulsive in nature. Lastly, the present study concluded that readied UADRS has higher adsorption limit esteem. Thus, UADRS can be successfully used as a minimal effort adsorbent for the removal of MG dye particles from the aquatic environment.

Table 4
Sticking probability of MG dye onto UADRS

Concentration of MG dye (mg L^{-1})	E_a (KJ mol^{-1})	S^*
50	–1.030	0.049
100	–0.543	0.208
150	–0.281	0.521
200	–0.253	0.719
250	–0.189	0.926

Table 5
Comparison of adsorption capacity of UADRS with other adsorbents for the adsorption of MG dye

S. No	Adsorbents	q_m (mg g^{-1})	References
1	UADRS	456.9	This study
2	Base-modified *Artocarpus odoratissimus* leaves	425.6	[48]
3	TEPFRCA	333.33	[49]
4	ZnO nanoparticles loaded activated carbon	322.6	[50]
5	Boron-doped mesoporous carbon nitride	310	[51]
6	Reduced graphene oxide-Agarose hydrogel	242	[52]
7	Groundnut shell derived activated carbon	222.2	[53]
8	CNF aerogel	212.7	[54]
9	Bentonite	178.6	[55]
10	Rice straw-derived char	148.6	[56]
11	Waste fruit residues	37.03	[57]
12	Wood apple shell	34.56	[58]
13	*Annona squamosa* seed	25.91	[59]
14	Cashew nut bark carbon	20.09	[60]
15	CPAC	4.4	[61]
16	Neem sawdust	4.354	[62]

References

[1] P.S. Kumar, M. Palaniyappan, M. Priyadharshini, A.M. Vignesh, A. Thanjiappan, S.A. Fernando, R.T. Ahmed, R. Srinath, Adsorption of basic dye onto raw and surface-modified agricultural waste, Environ. Prog. Sustainable Energy, 33 (2014) 87–98.

[2] A. Belbel, M. Kharroubi, J.-M. Janot, M. Abdessamad, A. Haouzi, I.K. Lefkaier, S. Balme, Preparation and characterization of homoionic montmorillonite modified with ionic liquid: application in dye adsorption, Colloids Surf., A, 558 (2018) 219–227.

[3] J.A. Kumar, D.J. Amarnath, P.S. Kumar, C.S. Kaushik, M.E. Varghese, A. Saravanan, Mass transfer and thermodynamic analysis on the removal of naphthalene from aqueous solution using oleic acid modified palm shell activated carbon, Desal. Wat. Treat., 106 (2018) 238–250.

[4] M. Joshi, R. Bansal, R. Purwar, Colour removal from textile effluents, Indian J. Fibre Text. Res., 29 (2004) 239–259.

[5] R.P.F. Melo, E.L. Barros Neto, M.C.P.A. Moura, T.N.C. Dantas, A.A.D. Neto, H.N.M. Oliveira, Removal of Reactive Blue 19 using nonionic surfactant in cloud point extraction, Sep. Purif. Technol., 138 (2014) 71–76.

[6] M. Siddique, R. Farooq, A. Khalid, A. Farooq, Q. Mahmood, U. Farooq, I.A. Raja, S.F. Shaukat, Thermal-pressure-mediated hydrolysis of Reactive Blue 19 dye, J. Hazard. Mater., 172 (2009) 1007–1012.

[7] M.A. Ahmad, R. Alrozi, Removal of malachite green dye from aqueous solution using rambutan peel-based activated carbon: equilibrium, kinetic and thermodynamic studies, Chem. Eng. J., 171 (2011) 510–516.

[8] G.D. Değermenci, N. Değermenci, V. Ayvaoğlu, E. Durmaz, D. Çakir, E. Akan, Adsorption of reactive dyes on lignocellulosic waste; characterization, equilibrium, kinetic and thermodynamic studies, J. Cleaner Prod., 225 (2019) 1220–1229.

[9] S. Srivastava, R. Sinha, D. Roy, Toxicological effects of malachite green, Aquat. Toxicol., 66 (2004) 319–329.

[10] D. Solís-Casados, L. Escobar-Alarcón, M. Fernández, F. Valencia, Malachite green degradation in simulated wastewater using Ni_2:TiO_2 thin films, Fuel, 110 (2013) 17–22.

[11] S. Raghu, C.A. Basha, Chemical or electrochemical techniques, followed by ion exchange, for recycle of textile dye wastewater, J. Hazard. Mater., 149 (2007) 324–330.

[12] J. Labanda, J. Sabaté, J. Llorens, Modeling of the dynamic adsorption of an anionic dye through ion-exchange membrane adsorber, J. Membr. Sci., 340 (2009) 234–240.

[13] S. Mondal, H. Ouni, M. Dhahbi, S. De, Kinetic modeling for dye removal using polyelectrolyte enhanced ultrafiltration, J. Hazard. Mater., 229–230 (2012) 381–389.

[14] M. Constantin, I. Asmarandei, V. Harabagiu, L. Ghimici, P. Ascenzi, G. Fundueanu, Removal of anionic dyes from aqueous solutions by an ion-exchanger based on pullulan microspheres, Carbohydr. Polym., 91 (2013) 74–84.

[15] V. Buscio, M. Crespi, C. Gutiérrez-Bouzán, Sustainable dyeing of denim using indigo dye recovered with polyvinylidene

difluoride ultrafiltration membranes, J. Cleaner Prod., 91 (2015) 201–207.
[16] M.C. Villalobos, A.A. Peláez Cid, A.M. Herrera González, Removal of textile dyes and metallic ions using polyelectrolytes and macroelectrolytes containing sulfonic acid groups, J. Environ. Manage., 177 (2016) 65–73.
[17] Y.Y. Ling, F.B.M. Suah, Extraction of malachite green from wastewater by using polymer inclusion membrane, J. Environ. Chem. Eng., 5 (2017) 785–794.
[18] M. Jiang, K.F. Ye, J.Y. Lin, X.Y. Zhang, W.Y. Ye, S.F. Zhao, B. Van der Bruggen, Effective dye purification using tight ceramic ultrafiltration membrane, J. Membr. Sci., 566 (2018) 151–160.
[19] K. Rambabu, G. Bharath, P. Monash, S. Velu, F. Banat, Mu. Naushad, G. Arthanareeswaran, P.L. Show, Effective treatment of dye polluted wastewater using nanoporous $CaCl_2$ modified polyethersulfone membrane, Process Saf. Environ. Prot., 124 (2019) 266–278.
[20] R. Jothirani, P.S. Kumar, A. Saravanan, A.S. Narayan, A. Dutta, Ultrasonic modified corn pith for the sequestration of dye from aqueous solution, J. Ind. Eng. Chem., 39 (2016) 162–175.
[21] V. Tharaneedhar, P.S. Kumar, A. Saravanan, C. Ravikumar, V. Jaikumar, Prediction and interpretation of adsorption parameters for the sequestration of methylene blue dye from aqueous solution using microwave assisted corncob activated carbon, Sustainable Mater.Technol., 11 (2017) 1–11.
[22] A. Saravanan, P.S. Kumar, M. Yashwanthraj, Sequestration of toxic Cr(VI) ions from industrial wastewater using waste biomass: a review, Desal. Wat. Treat., 68 (2017) 245–266.
[23] Z. Li, X. Meng, Z. Zhang, Equilibrium and kinetic modelling of adsorption of Rhodamine B on MoS_2, Mater. Res. Bull., 111 (2019) 238–244.
[24] A.M. Herrera-Gonzalez, M. Caldera-Villalobos, A.-A. Pelaez-Cid, Adsorption of textile dyes using an activated carbon and crosslinked polyvinyl phosphonic acid composite, J. Environ. Manage., 234 (2019) 237–244.
[25] R. Gayathri, K.P. Gopinath, P.S. Kumar, A. Saravanan, Antimicrobial activity of *Mukia maderasapatna* stem extract of jujube seeds activated carbon against gram-positive/gram-negative bacteria and fungi strains: application in heavy metal removal, Desal. Wat. Treat., 72 (2017) 418–427.
[26] M.A.M. Salleh, D.K. Mahmoud, W.A.W.A. Karim, A. Idris, Cationic and anionic dye adsorption by agricultural solid wastes: a comprehensive review, Desalination, 280 (2011) 1–13.
[27] S. Rangabhashiyam, N. Anu, N. Selvaraju, Sequestration of dye from textile industry wastewater using agricultural waste products as adsorbents, J. Environ. Chem. Eng., 1 (2013) 629–641.
[28] L.H. Wang, Application of activated carbon derived from 'waste' bamboo culms for the adsorption of azo disperse dye: kinetic, equilibrium and thermodynamic studies, J. Environ. Manage., 102 (2012) 79–87.
[29] Y. Zhou, L. Zhang, Z. Cheng, Removal of organic pollutants from aqueous solution using agricultural wastes: a review, J. Mol. Liq., 212 (2015) 739–762.
[30] M.J. Ahmed, Application of agricultural based activated carbons by microwave and conventional activations for basic dye adsorption: review, J. Environ. Chem. Eng., 4 (2016) 89–99.
[31] A. Saravanan, P.S. Kumar, B. Preetha, Optimization of process parameters for the removal of chromium(VI) and nickel(II) from aqueous solutions by mixed biosorbents (custard apple seeds and *Aspergillus niger*) using response surface methodology, Desal. Wat. Treat., 57 (2016) 14530–14543.
[32] P.S. Kumar, S.J. Varjani, S. Suganya, Treatment of dye wastewater using an ultrasonic aided nanoparticle stacked activated carbon: kinetic and isotherm modelling, Bioresour. Technol., 250 (2018) 716–722.
[33] K.H. Vardhan, R.C. Panda, A. Saravanan, Removal of Zn(II) ions from aqueous solution using chemically modified *Annona reticulata* seeds: kinetics, isotherm and thermodynamics, Desal. Wat. Treat., 122 (2018) 66–77.
[34] P.S. Kumar, S. Ramalingam, C. Senthamarai, M. Niranjanaa, P. Vijayalakshmi, S. Sivanesan, Adsorption of dye from aqueous solution by cashew nut shell: Studies on equilibrium isotherm, kinetics and thermodynamics of interactions, Desalination, 261 (2010) 52–60.
[35] P.S. Kumar, R. Sivaranjanee, U. Vinothini, M. Raghavi, K. Rajasekar, K. Ramakrishnan, Adsorption of dye onto raw and surface modified tamarind seeds: isotherms, process design, kinetics and mechanism, Desal. Wat. Treat., 52 (2014) 2620–2633.
[36] S. Charola, R. Yadav, P. Das, S. Maiti, Fixed-bed adsorption of Reactive Orange 84 dye onto activated carbon prepared from empty cotton flower agro-waste, Sustainable Environ. Res., 28 (2018) 298–308.
[37] N. Tahir, H.N. Bhatti, M. Iqbal, S. Noreen, Biopolymers composites with peanut hull waste biomass and application for Crystal Violet adsorption, Int. J. Biol. Macromol., 94 (2017) 210–220.
[38] Z. Jiang, D. Hu, Molecular mechanism of anionic dyes adsorption on cationized rice husk cellulose from agricultural wastes, J. Mol. Liq., 276 (2019) 105–114.
[39] P. Sathishkumar, M. Arulkumar, T. Palvannan, Utilization of agro-industrial waste *Jatropha curcas* pods as an activated carbon for the adsorption of reactive dye Remazol Brilliant Blue R (RBBR), J. Cleaner Prod., 22 (2012) 67–75.
[40] B. Shanmugarajah, I.M. Chew, N.M. Mubarak, T.S.Y. Choong, C. Yoo, K. Tan, Valorization of palm oil agro-waste into cellulose biosorbents for highly effective textile effluent remediation, J. Cleaner Prod., 210 (2019) 697–709.
[41] I. Langmuir, The adsorption of gases on plane surfaces of glass, mica and platinum, J. Am. Chem. Soc., 40 (1918) 1361–1403.
[42] H.M.F. Freundlich, Over the adsorption in solution, J. Phys. Chem., 57 (1906) 385–470.
[43] C. Aharoni, F.C. Tompkins, Kinetics of Adsorption and Desorption and the Elovich Equation, D.D. Eley, H. Pines, P.B. Weisz, Eds., Advances in Catalysis and Related Subjects, Academic Press, New York, 1970, pp. 21–22.
[44] J. Toth, Calculation of the BET-compatible surface area from any type I isotherms measured above the critical temperature, J. Colloid Interface Sci., 225 (2000) 378–383.
[45] S. Lagergren, About the theory of so-called adsorption of soluble substances, K. Sven. Vetenskapsakad. Handl., 24 (1898) 1–39.
[46] Y.S. Ho, G. McKay, Pseudo-second-order model for sorption processes, Process Biochem., 34 (1999) 451–465.
[47] M.J.D. Low, Kinetics of chemisorption of gases on solids, Chem. Rev., 60 (1960) 267–312.
[48] N.A.H.M. Zaidi, L.B.L. Lim, A. Usman, Enhancing adsorption of malachite green dye using base-modified *Artocarpus odoratissimus* leaves as adsorbents, Environ. Technol. Innovation, 13 (2019) 211–223.
[49] M. Ghasemi, S. Mashhadi, M. Asif, I. Tyagi, S. Agarwal, V.K. Gupta, Microwave-assisted synthesis of tetraethylene pentamine functionalized activated carbon with high adsorption capacity for Malachite green dye, J. Mol. Liq., 213 (2016) 317–325.
[50] M. Ghaedi, A. Ansari, M.H. Habibi, A.R. Asghari, Removal of malachite green from aqueous solution by zinc oxide nanoparticle loaded on activated carbon: kinetics and isotherm study, J. Ind. Eng. Chem., 20 (2014) 17–28.
[51] E.B. Azimi, A. Badiei, J.B. Ghasemi, Efficient removal of malachite green from wastewater by using boron-doped mesoporous carbon nitride, Appl. Surf. Sci., 469 (2019) 236–245.
[52] Y. Wang, P. Zhang, C.F. Liu, C.Z. Huang, A facile and green method to fabricate graphene-based multifunctional hydrogels for miniature-scale water purification, RSC Adv., 3 (2013) 9240–9246.
[53] S.-H. Huo, X.-P. Yan, Metal–organic framework MIL-100(Fe) for the adsorption of malachite green from aqueous solution, J. Mater. Chem., 22 (2012) 7449–7455.
[54] F. Jiang, D.M. Dinh, Y.-L. Hsieh, Adsorption and desorption of cationic malachite green dye on cellulose nanofibril aerogels, Carbohydr. Polym., 173 (2017) 286–294.
[55] E. Bulut, M. Ozacar, I.A. Sengil, Adsorption of malachite green onto bentonite: equilibrium and kinetic studies and process design, Microporous Mesoporous Mater., 115 (2008) 234–246.

[56] B.H. Hameed, M.I. El-Khaiary, Kinetics and equilibrium studies of malachite green adsorption on rice straw-derived char, J. Hazard. Mater., 153 (2007) 701–708.
[57] P. Parimaladevi, V. Venkateswaran, Kinetics, thermodynamics and isotherm modeling of adsorption of triphenylmethane dyes (methyl violet, malachite green and magenta ii) on to fruit waste, J. Appl. Technol. Environ. Sanit., 1 (2011) 273–283.
[58] A.S. Sartape, A.M. Mandhare, V.V. Jadhav, P.D. Raut, M.A. Anuse, S.S. Kolekar, Removal of malachite green dye from aqueous solution with adsorption technique using *Limonia acidissima* (wood apple) shell as low cost adsorbent, Arabian J. Chem., 10 (2017) S3229–S3238.
[59] T. Santhi, S. Manonmani, T. Smitha, Kinetics and isotherm studies on cationic dyes adsorption onto *Annona squamosa* seed activated carbon, Int. J. Eng. Sci. Technol., 2 (2010) 287–295.
[60] S. Parthasarathy, N. Manju, M. Hema, S. Arivoli, Removal of malachite green from industrial waste-water by activated carbon prepared from cashew nut bark Alfa Universal, Int. J. Chem., 2 (2011) 41.
[61] T.K. Arumugam, P. Krishnamoorthy, N.R. Rajagopalan, S. Nanthini, D. Vasudevan, Removal of malachite green from aqueous solutions using a modified chitosan composite, Int. J. Biol. Macromol., 128 (2019) 655–664.
[62] S.D. Khattri, M.K. Singh, Removal of malachite green from dye wastewater using neem sawdust by adsorption, J. Hazard. Mater., 167 (2009) 1089–1094.